# Kinetics of the Thermal Decomposition Mechanisms of Conducting and Non-conducting epoxy/Al Composites

## M. Azeem Arshad[1], A. Maaroufi[1,*], R. Benavente[2], G. Pinto[3]

[1]*University of Mohammed V Agdal, Laboratory of Composite Materials, Polymers and Environment, Department of Chemistry, Faculty of Sciences, Avenue Ibn Batouta, P.O.B. 1014, Rabat - Agdal, Morocco*
[2]*Instituto de Ciencia y Tecnología de Polímeros (CSIC), Juan de la Cierva, 3, 28006 Madrid, Spain*
[3]*Departamento de Ingeniería Química Industrial y del Medio Ambiente, E.T.S.I. Industriales, Universidad Politécnica de Madrid, 28006 Madrid, Spain*

## Abstract

This article reports a kinetic study of the thermal degradation of insulating/conducting epoxy/Al composites, in order to obtain their mechanistic information. A Comparison of thermo-analytical data obtained from epoxy/Al composites with pure epoxy under non-isothermal conditions, showed that aluminum affects the thermal behavior of epoxy complexly and the produced effect depends on the quantity of aluminum in epoxy. The influence of aluminum contents on the thermal degradation of epoxy was fairly explained on the basis of variations in catalytic activity and heat capacity of aluminum with temperature. Different differential and integral isoconversional methods were used to determine the activation energies and consequently the appropriate reaction model for the processes, which was found to be Šestâk-Berggren. Kinetic modeling satisfactorily simulated the thermal degradation rates of epoxy/Al composites in terms of their kinetic equations and suggested the possibility of weak interactions between epoxy and aluminum. The mechanistic information obtained by kinetic study was found in good agreement with SEM and XRD results.

*Keywords:* epoxy composites; aluminum; thermogravimetric analysis; thermal degradation; kinetics.

## 1. Introduction

Binary composites of polymers loaded with metals are highly used due to their hybrid nature i.e.; their electrical and thermal conductivities are comparable to metals while processing, optical and thermo-mechanical characteristics are analogous to polymers [1, 2]. They are suitable for numerous global applications such as conductive adhesives, photo-thermal/optical recorders, electroactive and smart materials. Indeed, the conductive nature in a polymer/metal composite arises as a result of the formation of multiple conducting chains between the dispersed phases (fillers) as the dispersion medium (matrix) is intrinsically insulator. At a certain amount of filler in matrix, no less than one connecting filler chain is available in the whole system, called percolation threshold. Below threshold, a bulk connecting component does not exist inside such type of systems; while above threshold, there exists a giant component of almost the order of system size. This transitional point is therefore considered a criterion above and below which two different structures of are available and those may impart the system significantly different properties [3, 4].

In our previous study, non-isothermal degradation kinetics of insulating/conducting epoxy/Zn composites was carried out [5] that has been very interesting to obtain comprehensive understanding of the thermal behaviors of these composites. In this study, kinetic modeling on insulating/conducting epoxy/Al composites will be performed and the information obtained from kinetic study will then be compared with those from structural analysis and interpreted. Aluminum is used in this study because it is nonpoisonous, abundant and cheap, light weight, good conductor and capable to exhibit self passivity. The linkage between epoxy and aluminum is also industrially important in view of the improvement of epoxy adhesion by the addition of aluminum [6]. Both the electrically insulating and conducting composites of polymer/Al are useful, e.g.; insulating composites are applied as thermal greases, thermal interface materials and electric cable insulations while, conductive composites are utilized in thermo-electrical/thermo-mechanical applications and solar cells [7, 8].

## 2. Experimental

*2.1.Formation of Composites*

The matrix used is diglycidyl ether of bisphenol-A (DGEBA/Epoxy F) with a hardener triethylene tetramine (HY956/Ciba-Geigy) whose structural formulae are given in Fig. 1.
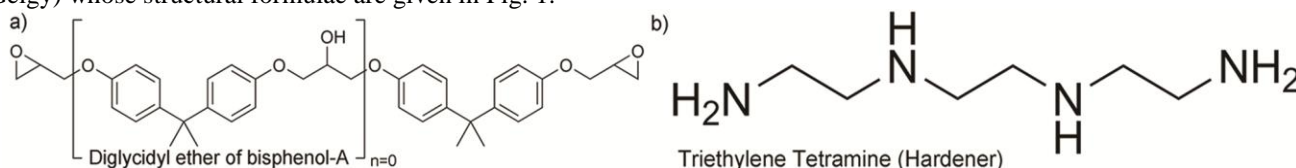


**Figure 1:** Structural formulae of a) diglycidyl ether of bisphenol-A (DGEBA) b) Triethylene tetramine

The polymer obtained has a density of 1.14 (g/cm$^3$) at 22°C. The filler is a commercial powder of aluminum, delivered by Panreac (Castellar del Vallès, Spain) with some of the characteristics which are listed in Table1.

**Table 1:** Physical characteristics of the metal used in the present study.

| Sample | Purity (%) | φ (μm) | d (g/cm$^3$) | ρ (μΩ.cm) |
|---|---|---|---|---|
| Aluminium | 98 | 30-70 | 2.70 | 2.653 |

All the composites have been prepared by employing the same procedure, as described elsewhere [5, 9]. Calculated quantities of metallic powder were introduced in the fluid resin and dispersed manually to obtain the homogeneity. The formed viscous suspension was flowed in Teflon mould casts and placed during one hour on the rotating rollers in oven maintained at 100°C. The mixture was rotated during polymerization process, so as to prevent the sedimentation of the particles whose densities are larger than that of polymeric ones. The possible curing reaction scheme for the formation of epoxy resin is given in Fig. 2 [10].
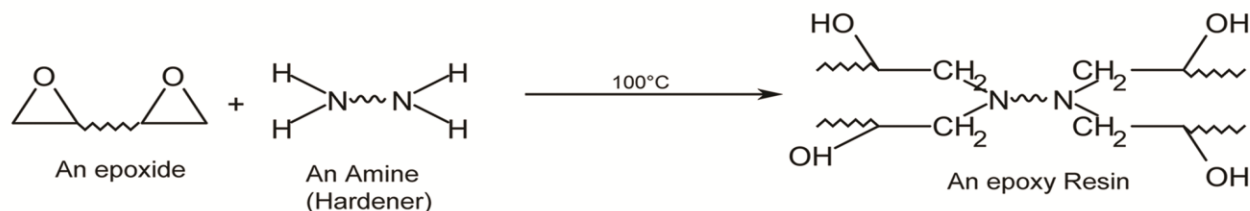


**Figure 2:** Curing reaction between DGEBA (Diglycidyl ether of bisphenol-A) and amine.

*2.2. Structural Characterization by SEM and XRD Analysis*

The dispersion of metallic particles in composite samples, their morphologies and polymer-metal interphases were analyzed by Philips XL30 scanning electron microscope with an accelerating voltage up to 20kV. This instrument is fully computer-controlled and equipped with an energy dispersive X-ray unit (EDX).

In order to evaluate the types of internal phases present inside pure epoxy and epoxy/Al composites, x-ray diffraction analysis was carried out by X'pert Pro diffractometer. Fairly thick and identical disk shaped samples having comparable dimensions were introduced in the diffractometer containing copper anode ($\lambda$=1.54Å) within the Bragg angle *2θ* $\epsilon$ (3°, 90°).

*2.3. Thermogravimetric Measurements*

In order to carry out the thermogravimetric analysis (TGA), an insulator/conductor pair of composites was selected above and below the percolation threshold (16.5% volume percent of Al) and was named epoxy/Al3vol.% and epoxy/Al30vol.%, respectively . The analysis was carried out by Q500 V20.0 TGA analyzer using dynamic experiment mode with $\beta$= 2, 5, 10, 15, 20, 25°C/min for pure epoxy and epoxy/Al composites from 30 to 600°C under 90ml/min of nitrogen flow.

## 3. Theory

*3.1. Kinetic Fundamentals*

In solid state kinetics, the extent of reaction is described by a term degree of conversion 'α' as following:

$$\alpha = \frac{m_0 - m_t}{m_0 - m_\infty} \tag{1}$$

Where, '$m_0$' is the initial mass of reactant, '$m_t$' is the mass at certain time during the reaction and '$m_\infty$' is the mass at the end of reaction. For these reactions, the reaction rate being the function of 'α' and temperature dependent rate constant suggest the following rate equation:

$$\frac{d\alpha}{dt} = A\exp(-E_\alpha / RT)f(\alpha) \tag{2}$$

Where, $d\alpha/dt$ is the reaction rate, $A$ is the pre-exponential factor, $E_\alpha$ is the activation energy as a function of 'α' (in calculations, an average value of energy '$E$' called effective energy is used), $T$ is the temperature, $f(\alpha)$ is the reaction model function and $R$ is gas constant. Eq. (2) is the basic kinetic equation of solid state reactions and a union of its parameters $A$, $E_\alpha$ and $f(\alpha)$ is known as the kinetic triplet [11].

### 3.2. Evaluation of Kinetic Triplet
Each and every member of kinetic triplet has its own physical meaning and relevant contribution towards the whole phenomenon. A number of methods are available in literature to evaluate them. Some of them are going to be explained in the following sections.

*3.2.1. Activation Energy Estimation by Isoconversional Methods*
Isoconversional methods are based upon the isoconversional principle which states that; "At constant extent of conversion, the rate of a solid state reaction depends only upon the temperature" [11]. Isoconversional methods can be isothermal/non-isothermal, differential/integral and linear/nonlinear. They are named so because they may be inter-convertible by certain multiples arising from numerical differentiation/integration of temperature integral and therefore generate analogous *E-α* dependency patterns [12].

*3.2.1.1. Differential Isoconversional Method: Freidman's Method*
Friedman's method is a well known differential isoconversional method [13] with the following general expression,

$$\ln(d\alpha / dt)_{\alpha,\beta} = -E_\alpha / RT_{\alpha,\beta} + \ln\{Af(\alpha)\} \tag{3}$$

The $E_\alpha$ values can be determined by plotting $ln(d\alpha/dt)$ against $1/T$ at a certain values of α which strictly demands numerical differentiation. The resulting $E_\alpha$ values could therefore be significantly irregular.

*3.2.1.2. Integral Isoconversional Methods*
A number of approximations applied to numerically solve the temperature integral [14] yield the following generalized linear integral isoconversional method:

$$\ln\left(\frac{\beta}{T_\alpha^{\,b}}\right) = Const. - \left(\frac{aE_\alpha}{RT_\alpha}\right) \tag{4}$$

In Eq. (4), '$a$' and '$b$' are constants which depend upon the employed method. For instance (a, b) = (1.052, 0) for OFW method [15] ; (a, b) = (1, 2) in case of Kissinger-Akahira-Sunose (KAS) method [16], etc. Eq. (4) represents an equation of straight line in the form $y=mx+c$ with $y=ln[\beta/T_\alpha^{\,b}]$, $x=1/T_\alpha$ and $m=-aE_\alpha/R$. The value of $E_\alpha$ at each value of $\alpha$ can be calculated by the slopes of straight lines.

*3.2.2. Reaction Model Determination*
The reaction model is a mathematical function of the extent of conversion which could furnish the information about reaction pathway(s). A relatively efficient method to determine the reaction models of thermally stimulated solid state reactions was proposed by Malék [17]. An average value of activation energy from isoconversional methods should be known as a preliminary condition and then a pair of functions $y(\alpha)$ and $z(\alpha)$ can be constructed to access the reaction model and its parameter(s) as shown in Eqs. (5)-(6) respectively:

$$y(\alpha) \approx (d\alpha / dt)\exp(x) \tag{5}$$

$$z(\alpha) \approx \pi(x)(d\alpha / dt)T / \beta \tag{6}$$

In Eq. (6), $\pi(x)$ is a function of temperature integral with $x=E/RT$. A relatively more precise numerical approximation of $\pi(x)$ was suggested by Senum and Yang [18] and corrected by Flynn [12] as shown in Eq. (7).

$$\pi(x) = \frac{x^4 + 18x^3 + 86x^2 + 96x}{x^4 + 20x^3 + +120x^2 + 240x + 120} \tag{7}$$

The maxima $(\alpha_M, \alpha_p^\infty)$ of $y(\alpha)$ and $z(\alpha)$ functions respectively and '$\alpha_p$' being the degree of conversion at maximum reaction rate, are helpful to evaluate the appropriate reaction model for a certain reaction, according to the conditions set by Malék [17]. Once the activation energy and reaction model are known, pre-exponential factor can easily be determined by Eq. (2).

## 4. Results and Discussion
### 4.1. SEM and XRD Results
The results obtained by performing cross sectional SEM analysis, following the conditions described in experimental section, have been shown in Fig. 3.
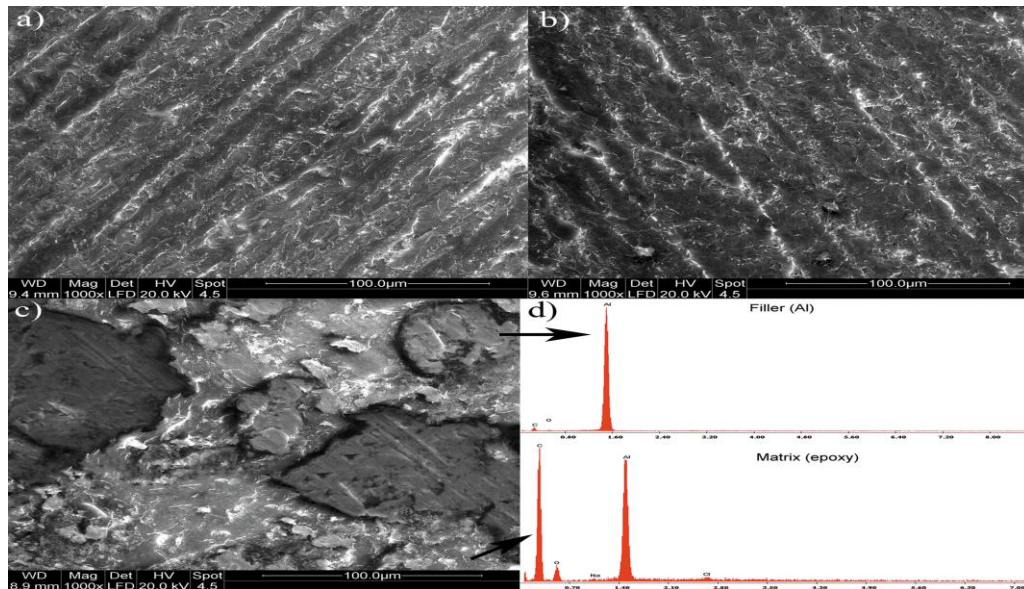
**Figure 3:** Cross sectional SEM micrographs a) pure epoxy b) epoxy/Al3vol.% c) epoxy/Al30vol.% d) EDX of epoxy/Al30vol.%

The lines observed in Fig. 3a-b are due to the surface treatments for SEM observations. Fig. 3a-c represents the morphologies of pure epoxy, epoxy/Al3vol.% and epoxy/Al30vol.% composites, respectively. SEM analysis of Fig.3a shows almost phase homogeneity in pure epoxy. Fig. 3b-c also depicts the uniform distribution of aluminum particles inside epoxy. Therefore, the epoxy and epoxy/Al composites can be considered fairly homogeneous. The epoxy-Al interphase is visible in Fig. 3c, showing some interactions between polymer and filler. Fig. 3d describes the EDX plot of Al and epoxy in epoxy/Al30vol.% composite. The principle peaks are due to the aluminum and carbon in composites. In addition, the peaks of Na, Cl, etc. are weak indicating their presence as contaminations. The comparative diffractograms of pure epoxy, epoxy/Al3vol.% and epoxy/Al30vol.% composites are shown in Fig. 4.
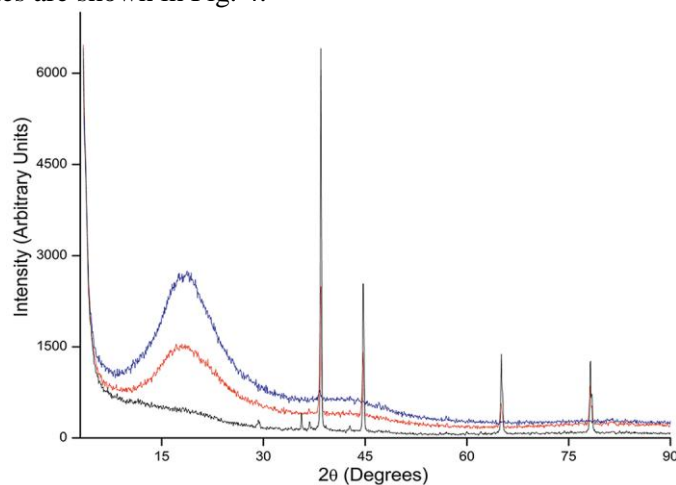


**Figure 4:** X-ray diffractograms of pure epoxy, epoxy/Al3vol.%  and epoxy/Al30vol.%.

A single broad peak of pure epoxy at $2\theta \approx 19°$ shows the amorphous nature of polymeric matrix. In case of epoxy/Al3vol.% and epoxy/Al30vol.%, four peaks of different intensities are visible at 38.46°, 44.75°, 65.1° and 78.23°. The peaks available at 38.46°, 44.75°, 65.1° could be attributed to centered cubic/face centered cubic geometries of Al and/or $Al_2O_3$ (due to partial oxidation of filler) [19]. In addition to these peaks, an explicit peak is observed around 78° in epoxy/Al composites but it is absent in pure epoxy. This peak might correspond to the interactions between epoxy and aluminum in composites, resulting in the formation of a crystalline organo-metallic complex/chelate. Such phenomenon has already been observed in the formation of epoxy–amine/metal interphases [20].

*4.2. Effect of nature and contents of Al on Thermal Degradation of epoxy*

The percentage mass loss values and normalized derivatives of reactant mass as a function of temperature, generated by Q500 V20.0 TGA analyzer under the conditions described in experimental section for pure epoxy, epoxy/Al3vol.% and epoxy/Al30vol.% are represented in Fig. 5a-c respectively.
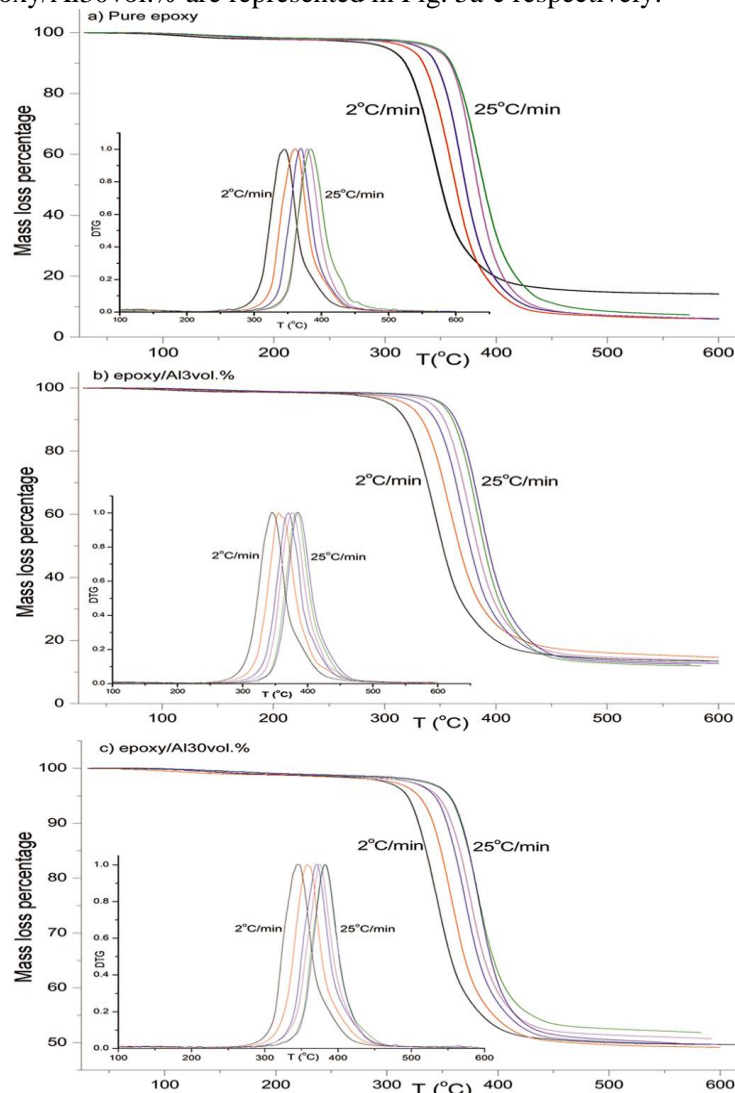


**Fig. 5:** Typical TGA and DTG (inset) curves at different β values a) pure epoxy b) epoxy/Al3vol.% c) epoxy/Al30vol.%

The nature of degradation process is usually determined by the shape and position of TGA curve and the width of DTG peak which is constituent specific. Fig. 5a shows that the mass loss of epoxy is smooth between 30°C to 300°C which could be attributed to the scission of weaker linkages like, dehydration of resin, intermolecular/intramolecular hydrogen bonding and/or polymer-polymer/polymer-metal interactions present in it as already shown [5]. However, the true degradation region lies between 300-450°C which could be assigned to the breakage of 3D cross linked network and linear C-C chains in the polymer. Phenol and bisphenol-A have been found as the major pyrolytic fractions in this range [21]. The degradation behavior of epoxy/Al composites seems similar to the pure epoxy as been observed in Fig. 5b-c. Fig. 6a shows that aluminum has the ability to enhance the thermal stability of epoxy and the enhancement in stability of epoxy seems a function of aluminum contents in epoxy. The increase in the thermal stability of epoxy by the addition of aluminum has already been cited in the literature [22, 23]. Although, this behavior is strictly apparent or virtual since these TGA curves include also the mass of filler known as uncorrected TGA curves.

In order to find the actual effect of Al on the epoxy, the mass of Al was subtracted from the apparent mass of composite at each relevant temperature and the percentage mass loss of epoxy along with the corrected TGA curves of epoxy/Al composite were drawn as a function of temperature at 10°C/min as shown in corrected TGA curves in Fig. 6b. The corrected TGA curves in Fig. 6b show interesting phenomenon. The trend of thermal

stabilities of epoxy/Al composites relative to pure epoxy becomes irregular as been remarked in corrected TGA curves in Fig. 6b. The aluminum contents in epoxy tends to accelerate the degradation of epoxy at relatively lower temperatures and then commence stabilizing the matrix. In view of verifying this behavior, the logarithmic plots of characteristic decomposition temperatures; initial decomposition temperature ($T_i$), temperature at maxima of DTG peak ($T_m$) and final decomposition temperature ($T_f$) of pure epoxy and epoxy/Al composites against heating rates in uncorrected and corrected TGA curves, are shown in Fig. 7a and 7b, respectively.
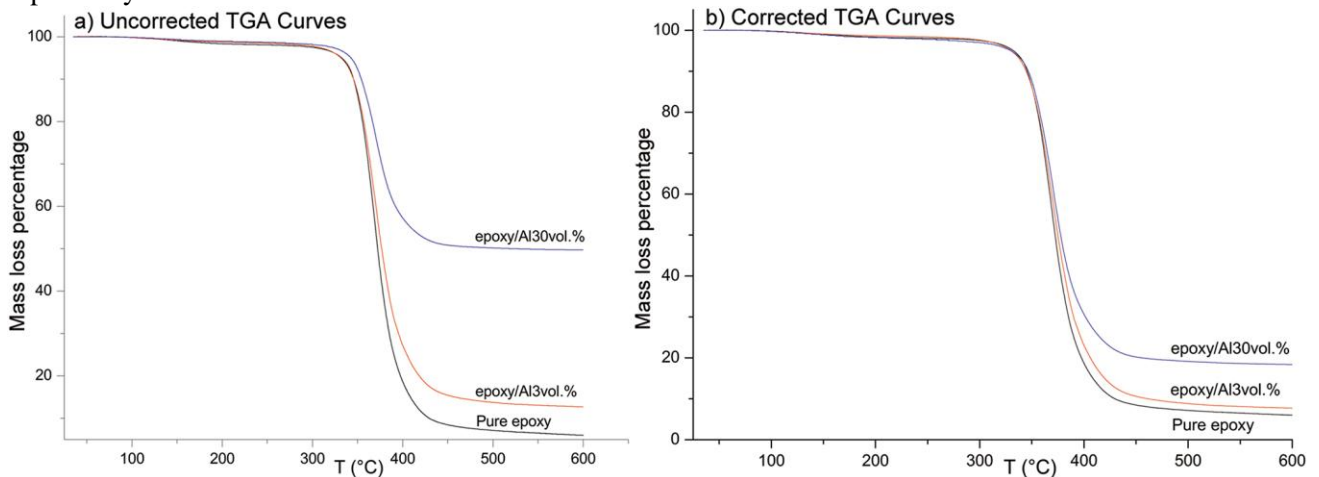


**Figure 6:** a) Uncorrected TGA curves of pure epoxy, epoxy/Al3vol.%  and epoxy/Al30vol.%
b) Corrected TGA curves of pure epoxy, epoxy/Al3vol.%  and epoxy/Al30vol.%, at 10°C/min

The data obtained from the linear fits of the graphs shown in Fig.7a-b has been pasted in Tables 2-3. It is obvious from Table 2 that the apparent effect induced by aluminum to epoxy is stabilizing at the initial and final stages of reaction since the logarithmic rate of change in characteristic decomposition temperatures ($T_i$ and $T_f$ ) with respect to $\beta$ is highest for epoxy/Al30vol.%, intermediate for epoxy/Al3vol.% and lowest for pure epoxy.



**Figure 7:** a) Variation in $lnT_i$, $lnT_m$, $lnT_f$, with $ln\beta$ in case of pure epoxy, epoxy/Al3vol.%  and epoxy/Al30vol.% obtained from uncorrected TGA c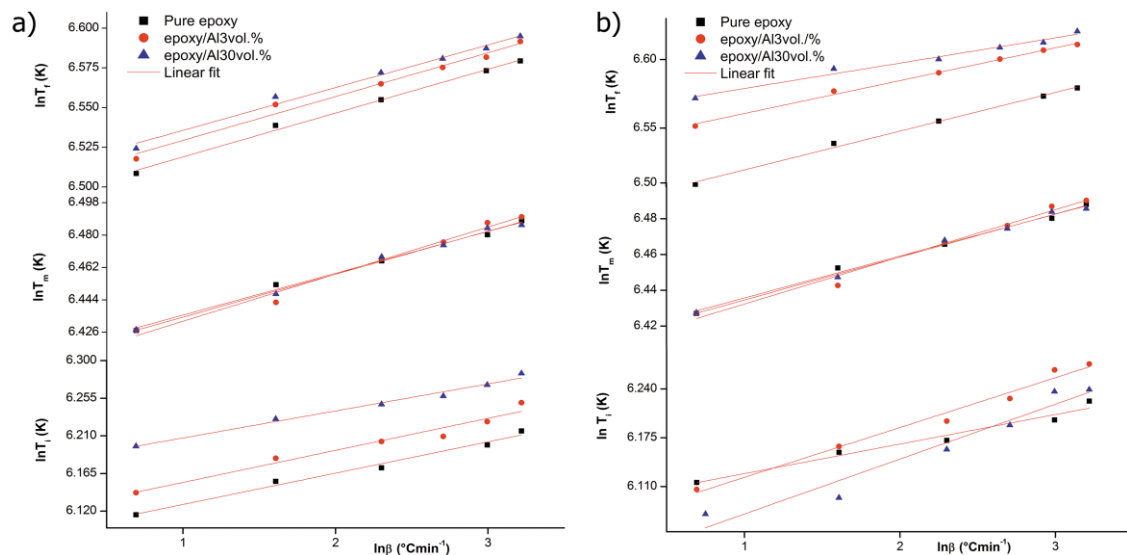urves; b) Variation in $lnT_i$, $lnT_m$, $lnT_f$, with $ln\beta$ in case of pure epoxy, epoxy/Al3vol.%  and epoxy/Al30vol.% obtained from corrected TGA curves .

At the maxima of reaction rate, the logarithmic rate of change in $T_m$ with respect to $\beta$ shows that the behavior of epoxy/Al3vol/% is slightly more accelerating the reaction in comparison with pure epoxy and epoxy/Al30vol.% which show comparable rates. However, the actual effect of aluminum contents produced on epoxy can be seen in the data obtained from corrected TGA curves in Table 2. These data show that the aluminum may speed up

the reaction in the initial stages and this increase could be a function of aluminum contents in epoxy; although, at the final stages of reaction, the increasing contents of aluminum may provide resistance to the degradation of epoxy. At the intermediate reaction stages, the behavior shown by uncorrected and corrected TG curves remains almost the same. These observations can be confirmed by the comparison of $T_i$, $T_m$ and $T_f$ values of pure epoxy and epoxy/Al composites at $\beta = 1°C/min$, obtained by the intercepts of straight lines of the plots in Fig.7a-b as shown in Table 3.

The influence of nature and contents of aluminum on the thermal degradation behavior of epoxy may be explained on the basis of competitive effect of the catalytic activity and heat capacity of aluminum and the their variations with temperature on epoxy. Like iron [24] and zinc [5], aluminum may accelerate the degradation rate of epoxy by catalyzing the reaction. Yet, aluminum is catalytically more efficient at lower temperatures and its catalytic activity is reduced at higher temperatures as a result of catalytic deactivation [25]. Moreover, the heat capacity of metals depends upon their masses and the temperature. The heat capacity of aluminum varies from $0.893 Jg^{-1}K^{-1}$ to $1.179$ $Jg^{-1}K^{-1}$ when temperature changes from 30°C to 600°C which is responsible to absorb more heat and thus provides shield against thermal degradation of epoxy [26, 22].

**Table 2:** Comparison between $dT_i/dln\beta$, $dT_m/dln\beta$ and $dT_f/dln\beta$ values for pure epoxy, epoxy/Al3vol.% and epoxy/Al30vol.% obtained from uncorrected and corrected TG curves.

| Data from Uncorrected TG Curves | | | | | | Data from Corrected TG Curves | | | | | |
|---|---|---|---|---|---|---|---|---|---|---|---|
| Sample | $dT_i/dln\beta$ | $r^2$ | $dT_m/dln\beta$ | $r^2$ | $dT_f/dln\beta$ | $r^2$ | Sample | $dT_i/dln\beta$ | $r^2$ | $dT_m/dln\beta$ | $r^2$ | $dT_f/dln\beta$ | $r^2$ |
| Pure epoxy | 0.0393 | 0.985 | 0.0233 | 0.992 | 0.0275 | 0.994 | Pure epoxy | 0.0393 | 0.985 | 0.0233 | 0.992 | 0.0275 | 0.994 |
| epoxy/Al3vol.% | 0.0383 | 0.961 | 0.0261 | 0.987 | 0.0275 | 0.985 | epoxy/Al3vol.% | 0.0663 | 0.979 | 0.0262 | 0.986 | 0.0233 | 0.995 |
| epoxy/Al30vol.% | 0.0323 | 0.982 | 0.024 | 0.992 | 0.0268 | 0.987 | epoxy/Al30vol.% | 0.0731 | 0.951 | 0.0239 | 0.995 | 0.0180 | 0.981 |

Taking into account these properties of aluminum, it can be said that the net effect of aluminum on the thermal degradation of epoxy is catalyzing at relatively lower temperatures because the heat capacity of aluminum is low at those temperatures; also, this effect may increase by increasing the loadings of aluminum into epoxy. However, at higher temperatures, the catalytic activity of aluminum is reduced and its specific heat is very high which results in the significant thermal stability of epoxy. The thermal stability of epoxy is improved at higher temperatures as the amount of aluminum in it is enhanced. At intermediate stages of reaction, the thermal degradation rate of epoxy and epoxy/Al composites might be considered comparable since the effects of catalytic activity and heat capacity of aluminum may counteract each other at those temperatures.

**Table 3:** $T_i$, $T_m$ and $T_f$ values of pure epoxy, epoxy/Al3vol.% and epoxy/Al30vol.% obtained at $\beta = 1°Cmin^{-1}$ from the intercepts of linear fits as shown in Fig. 7a & 7b.

It is worthy to notice in Fig. 7a-b that the linear fits intersect each other at a point ($\beta = 6.7°C/min$, $T_m = 636.76K/363.61°C$). It probably means that the pure epoxy and epoxy/Al composites degrade with the similar rates around heating rate 6.7°C/min with a temperature 363.61°C relevant to the maxima of DTG peak.

| Data from Uncorrected TG Curves | | | | Data from Corrected TG Curves | | | |
|---|---|---|---|---|---|---|---|
| Sample | $T_i$ (°C) | $T_m$ (°C) | $T_f$ (°C) | Sample | $T_i$ (°C) | $T_m$ (°C) | $T_f$ (°C) |
| Pure epoxy | 168.65 | 336.3 | 386.43 | Pure epoxy | 168.65 | 336.3 | 386.43 |
| epoxy/Al3vol.% | 180.05 | 332.4 | 393.35 | epoxy/Al3vol.% | 153.63 | 332.19 | 417.1 |
| epoxy/Al30vol.% | 207.64 | 335.25 | 401.36 | epoxy/Al30vol.% | 130.59 | 335.11 | 433.66 |

*4.3. Thermal Degradation Kinetics*

A satisfactory explanation of the thermal degradation behaviors of epoxy/Al composites is furnished by the kinetic study of this phenomenon. As each and every isoconversional method has a certain error associated with it, a set of three differential and integral methods of Friedman, KAS and OFW has been used within the α-

domain [.05, .95] with *Δα* = .05. Fig. 8A-C shows the results obtained by applying the same set of isoconversional methods to pure epoxy, epoxy/Al3vol.% and epoxy/Al30vol.% respectively. A slight non linear behavior at the extremities is observed for KAS and OFW methods, which becomes intense for Friedman's method due to the noisy points. Fig. 9a-c represents the comparison of *E* values obtained by different methods against α for pure epoxy, epoxy/Al3vol.% and epoxy/Al30vol.%, respectively.
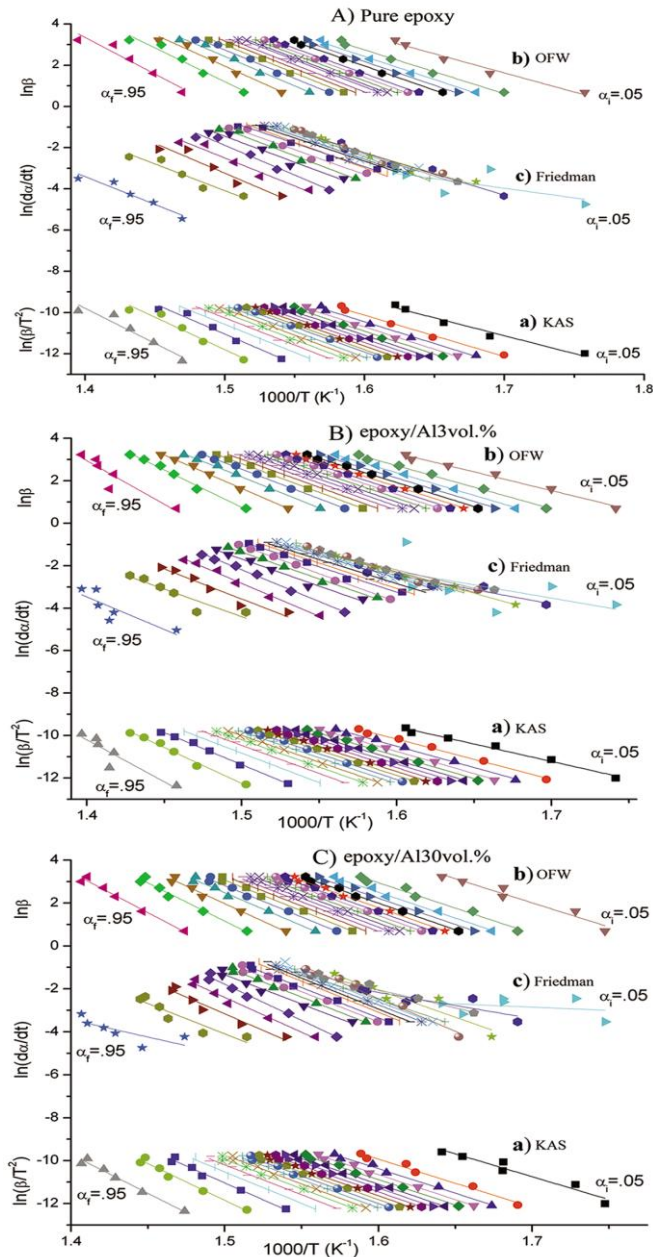


**Figure 8:** Applications of isoconversional methods to the non-isothermal degradation of the materials with a) KAS b) OFW and c) Friedman's method A) pure epoxy  B) epoxy/Al3vol.%  C) epoxy/Al30vol.%

The variation in $E_\alpha$ with *α* has been found analogous in each case neglecting the numerical differentiation error usually appears in Friedman's method [11, 14]. The average *E* values of pure epoxy, epoxy/Al3vol.% and epoxy/Al30vol.% are taken by considering E-α dependency plots of KAS and OFW methods which have been represented in Table 4.

**Table 4:** Average E values of pure epoxy, epoxy/Al3vol.% and  epoxy/Al30vol.%.

| Sample | Pure epoxy | epoxy/Al3vol.% | epoxy/Al30vol.% |
|---|---|---|---|

| Average E (kJ/mol) | 202±11 | 196±14 | 211±12 |
|---|---|---|---|

### 4.3.1. Explanation of E-α Dependencies

The variation in activation energy during a solid state reaction is common and a controversial issue in thermal analysis [27]. The reactions of epoxy resins can be taken as a clear example [28]. Obviously, three different regions can be marked in each case of pure epoxy and epoxy/Al composites, as shown in Fig. 9a-c. The first region ranges from 0 to .2 of α provides information about initial mass loss that could be due to the volatile components and/or interactions present in macromolecular structure, as discussed in the earlier section. The $E_\alpha$ values are fairly stable in 2$^{nd}$ region within (0.2, 0.8) which could be due to the principal curing reaction between epoxy and amine. The 3$^{rd}$ region is found within (0.8, 1) representing an abrupt change in $E$ values which can be referred to the breakage of strong linkages of linear chain. The reaction under consideration seems to involve at least two different competitive reaction pathways [29]. A similar pattern of the variance in $E_\alpha$ with α has been seen in the kinetic study of biodegradable polyester poly (propylene suberate) [30], epoxy/silica composites [31], epoxy/Zn composites [5] and epoxy/Fe composites [24].
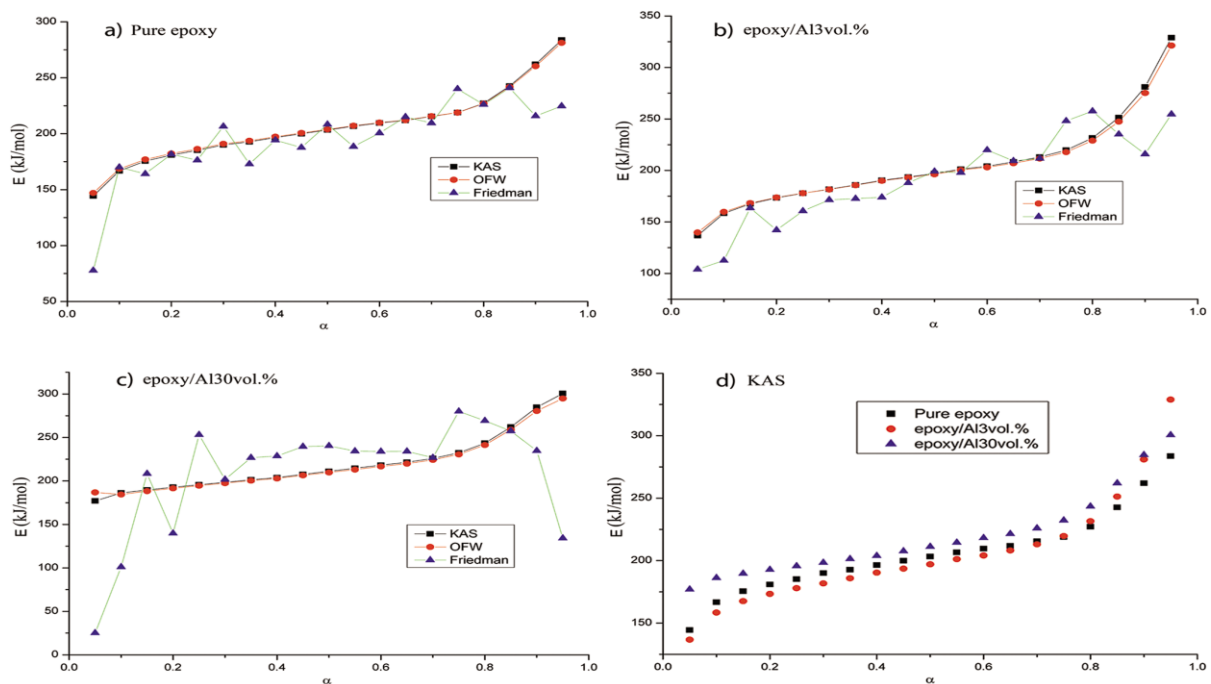


**Figure 9:** E-α dependency derived from isoconversional methods a) pure epoxy
b) epoxy/Al3vol.% c) epoxy/Al30vol.% d) E-α dependency comparison by KAS method

Fig. 9d compares the E-α dependencies of pure epoxy and epoxy/Al composites by KAS method. It could be said that the minute quantity of aluminum in epoxy may lower the energy barrier of resulting epoxy/Al3vol% composite; while, large quantity of aluminum may enhance the energy barrier of epoxy/Al30vol.% composite since,$(E_{epoxyAl3\%})_{av.}$=195.84±14kJ/mol and $(E_{epoxyAl30\%})_{av.}$= 210.76±12kJ/mol in comparison with $(E_{epoxy})_{av.}$=201.49±11kJ/mol.

### 4.3.2. Determination of Reaction Models and Kinetic Expressions

The normalized $z(\alpha)$ and $y(\alpha)$ functions and reaction rates within [0,1] as a function of α can be generated by applying Eqs. (5)-(6) to the experimental data as been shown in Fig. 10a-c for pure epoxy, epoxy/Al3vol.% and epoxy/Al30vol.% respectively. Variation in reaction rate against the degree of conversion for pure epoxy at different heating rates is given in Fig.10d. The variations in reaction rates of epoxy/Al composites as a function of α, are analogous to pure epoxy.
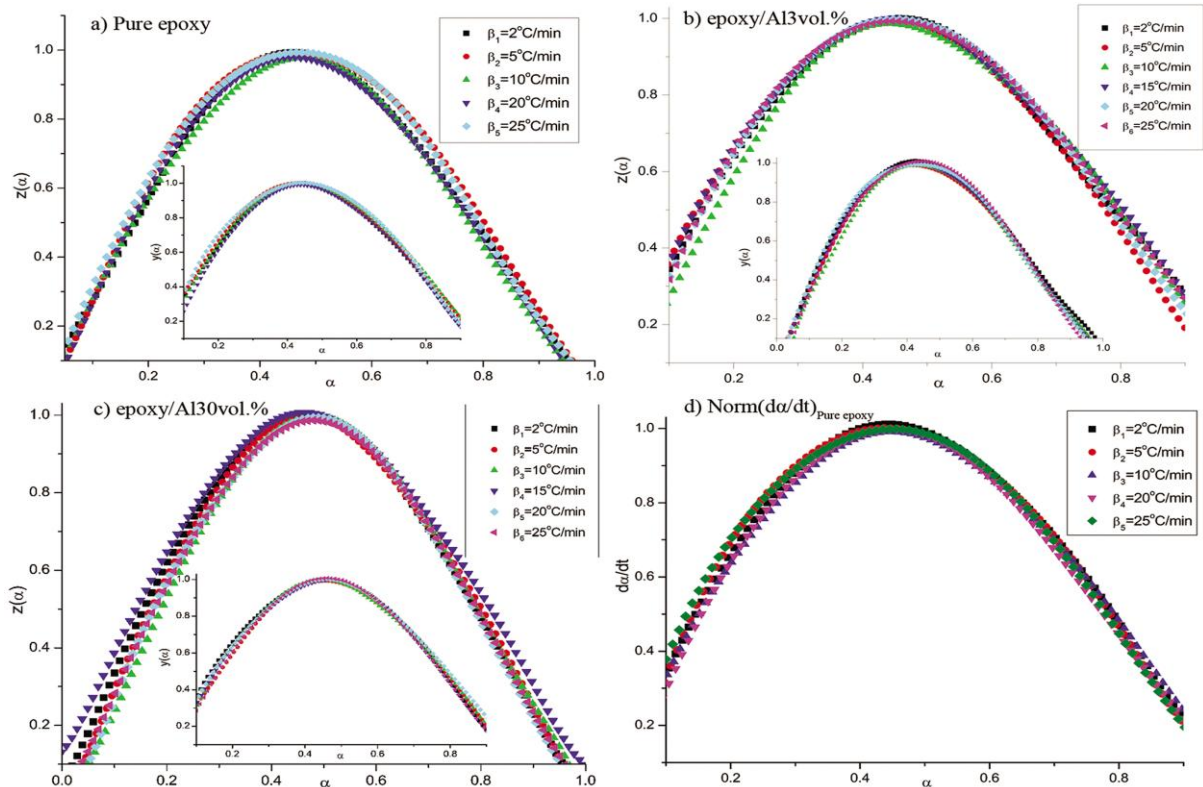
**Figure 10:** *z(α)* and *y(α)* (inset) against *α* at different *β* values a) pure epoxy  b) epoxy/Al3vol.% c) epoxy/Al30vol.%  d) Normalized reaction rate of pure epoxy against *α* at different *β* values.

The obtained values of $\alpha_p^\infty$, $\alpha_M$ and $\alpha_p$ values for pure epoxy, epoxy/Al3vol.% and epoxy/Al30vol.% has been shown in Table 5. A comparison of the set ($\alpha_p^\infty$, $\alpha_M$, $\alpha_p$) for epoxy and epoxy/Al composites suggests that the thermal degradation kinetics of epoxy and epoxy/Al composites can be best described by two parameter autocatalytic Šestâk Berggren model [32] since $\alpha_p^\infty \neq 0.623$ (condition for JMA model) and $\alpha_p^\infty > \alpha_p > \alpha_M$ [28]. Rearrangement of Eq. (2) yields Eq. (8),

$$\frac{d\alpha}{dt} = A \exp(-E/RT)(\alpha)^m (1-\alpha)^n \tag{8}$$

**Table 5:** Comparison of $\alpha_p^\infty$, $\alpha_M$ and $\alpha_p$ values for pure epoxy, epoxy/Al3vol.% and epoxy/Al30vol.%.

| Sample | Pure epoxy | | | epoxy/Al3vol.% | | | epoxy/Al30vol.% | | |
|---|---|---|---|---|---|---|---|---|---|
| Heating Rate (β) | $\alpha_p^\infty$ | $\alpha_M$ | $\alpha_p$ | $\alpha_p^\infty$ | $\alpha_M$ | $\alpha_p$ | $\alpha_p^\infty$ | $\alpha_M$ | $\alpha_p$ |
| 2 | 0.519 | 0.419 | 0.476 | 0.498 | 0.473 | 0.480 | 0.502 | 0.467 | 0.493 |
| 5 | 0.530 | 0.450 | 0.476 | 0.479 | 0.455 | 0.480 | 0.504 | 0.477 | 0.493 |
| 10 | 0.492 | 0.459 | 0.471 | 0.502 | 0.475 | 0.475 | 0.505 | 0.482 | 0.492 |
| 15 | ….. | ….. | ….. | 0.498 | 0.456 | 0.472 | 0.492 | 0.472 | 0.492 |
| 20 | 0.498 | 0.430 | 0.497 | 0.505 | 0.455 | 0.472 | 0.498 | 0.459 | 0.477 |
| 25 | 0.487 | 0.437 | 0.468 | 0.495 | 0.462 | 0.470 | 0.503 | 0.462 | 0.489 |
| Average | 0.506 | 0.439 | 0.478 | 0.496 | 0.463 | 0.475 | 0.50 | 0.470 | 0.489 |

Let '*p*' be the ratio of the reaction model parameters, as defined in Eq. (9),

$$p = \frac{m}{n} = \frac{\alpha_M}{1-\alpha_M} \tag{9}$$

Substituting the value of '*p*' from Eq. (9) into Eq. (8) and then rearranging Eq. (8) gives,

$$\ln\left\{\frac{d\alpha}{dt}\exp(E/RT)\right\} = \ln A + n\ln\left\{(\alpha)^{p}(1-\alpha)\right\} \qquad (10)$$

The plot of *ln[exp(E/RT)dα/dt]* against *ln[(α)$^p$(1- α)]* employing Eq. (10) appears a straight line whose slope and intercept provide the values of 'n' and 'lnA' respectively within (0,1) at each heating rate. The *m, n* and *lnA* values for pure epoxy, epoxy/Al3% and epoxy/Al30% are shown in Table 6.

**Table 6:** Comparison of *m*, *n* and *lnA* for pure epoxy, epoxy/Al3vol.%  and epoxy/vol.30%.

| Sample | Pure epoxy | | | | epoxy/Al3vol.% | | | | epoxy/Al30vol.% | | | |
|---|---|---|---|---|---|---|---|---|---|---|---|---|
| Heating Rate (β) | p | n | m | lnA | p | n | m | lnA | p | n | m | lnA |
| 2 | 0.723 | 2.57 | 2.02 | 39.3 | 0.899 | 3.56 | 3.07 | 38.94 | 0.876 | 2.4 | 2.12 | 40.35 |
| 5 | 0.818 | 3.64 | 2.85 | 40.36 | 0.849 | 3.86 | 3.33 | 39.48 | 0.914 | 3.15 | 2.79 | 41.19 |
| 10 | 0.851 | 3.54 | 2.77 | 40.53 | 0.907 | 3.12 | 2.69 | 38.54 | 0.931 | 3.11 | 2.75 | 41.1 |
| 15 | ….. | ….. | ….. | ….. | 0.838 | 3.37 | 2.9 | 38.99 | 0.893 | 3.11 | 2.76 | 41.35 |
| 20 | 0.754 | 2.77 | 2.17 | 39.58 | 0.836 | 2.96 | 2.55 | 38.31 | 0.851 | 3.33 | 2.96 | 41.74 |
| 25 | 0.775 | 2.99 | 2.35 | 39.57 | 0.858 | 2.46 | 2.11 | 37.34 | 0.859 | 2.95 | 2.7 | 41.34 |
| Average | 0.784 | 3.1 | 2.43 | 39.87 | 0.862 | 3.07 | 2.77 | 38.6 | 0.887 | 3.00 | 2.75 | 41.17 |

The substitution of the mean values of E, *m, n* and *A* in Eq. (8) generates the following explicit kinetic equations:

$$\left(\frac{d\alpha}{dt}\right)_{pure\ epoxy} = 2.1\times10^{17}\exp(-201490/RT)(\alpha)^{2.43}(1-\alpha)^{3.1} \qquad (11)$$

$$\left(\frac{d\alpha}{dt}\right)_{epoxy/Al3vol.\%} = 0.58\times10^{17}\exp(-195840/RT)(\alpha)^{2.77}(1-\alpha)^{3.07} \qquad (12)$$

$$\left(\frac{d\alpha}{dt}\right)_{epoxy/Al30vol.\%} = 7.6\times10^{17}\exp(-210760/RT)(\alpha)^{2.75}(1-\alpha)^{3} \qquad (13)$$

While, the kinetic equations already derived [5] for insulating/conducting epoxy/Zn composites are given below;

$$\left(\frac{d\alpha}{dt}\right)_{epoxy/Zn3vol.\%} = 8.7\times10^{15}\exp(-186235/RT)(\alpha)^{2.5}(1-\alpha)^{2.87} \qquad (14)$$

$$\left(\frac{d\alpha}{dt}\right)_{epoxy/Zn29vol.\%} = 1.3\times10^{16}\exp(-186154/RT)(\alpha)^{2.53}(1-\alpha)^{2.9} \qquad (15)$$

Fig. 11a-c shows a fair agreement between the experimental data and proposed kinetic Eqs. (11)-(13) for pure epoxy, epoxy/Al3vol.% and epoxy/Al30vol.% respectively, in terms of the variation of their reaction rates with temperature.

*4.4. Prediction of Reaction Mechanism*
 The comparison of kinetic equations of pure epoxy and epoxy/Al composites can give some useful information about the alteration of the kinetic triplets of composites and therefore their reaction mechanisms. Kinetic Eqs. (11)-(13) suggest Ŝestàk Berggren model for thermal degradation of epoxy and epoxy/Al composites which may accommodate different mechanisms under certain ranges of its parameters. The mechanism of a reaction can be satisfactorily proposed by employing this model if *m≤1*; moreover, the greater values of *m* and *n* depict the increasing complexity of reaction [33]. Actually, SB (*m, n*) model is a more generalized case of Prout-Tompkin equation [34] which is based upon the logistic function to model the relative population growth of molecules in materials.
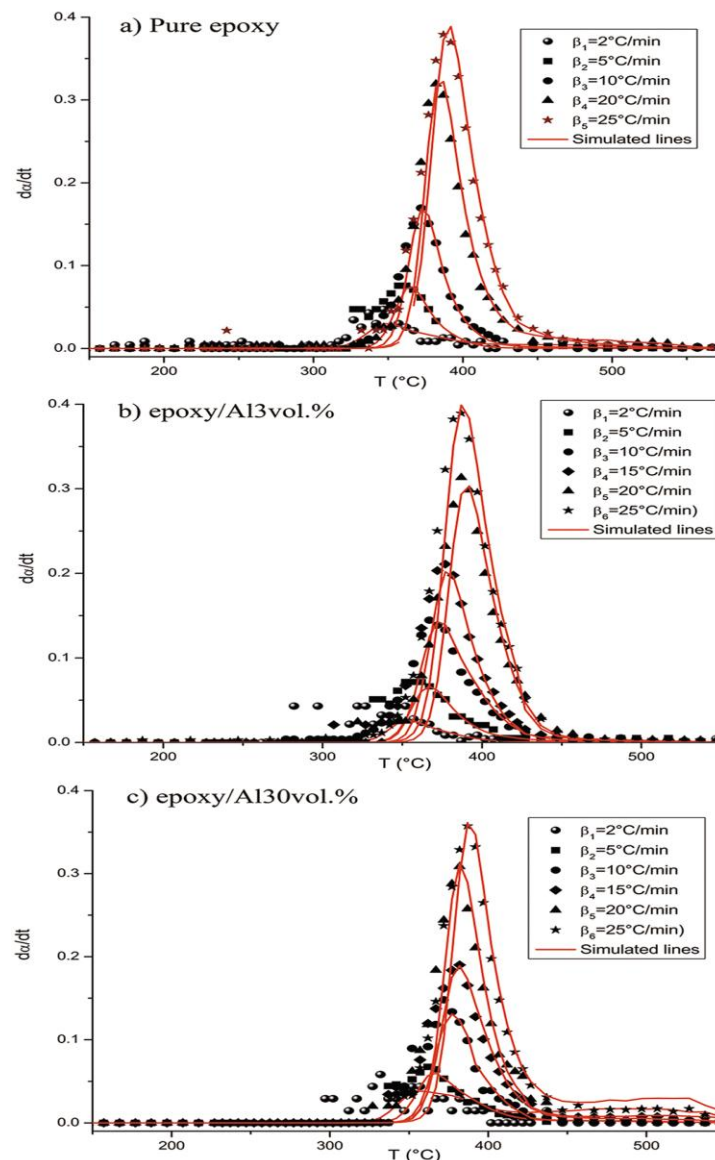
**Fig.11:** Agreement between theoretical and experimental data at different *β* values a) pure epoxy
b) epoxy/Al3vol.% c) epoxy/Al30vol.%.

The higher values of *m* and *n* in SB model might be assigned to the simultaneous occurrence of nucleation and growth phenomena, respectively [32]. A brief comparison of Eqs. (11)-(13) shows that the nucleation phenomenon is rapid in all epoxy and its composites and it remains independent of the introduction of aluminum into it. Aluminum probably participates in the formation of 3D network of epoxy by catalyzing the reaction; although its catalytic activity reduces at higher temperatures. An interesting phenomenon is observed while comparing the relative influences of zinc and aluminum contents on epoxy in Eqs. (11)-(15). It has already been mentioned that the polymer-metal interactions in case of epoxy/Zn composites are negligible which can be remarked in Eqs. (14)-(15) that the reaction model is independent of introducing zinc to epoxy [5]. However, aluminum interacts with epoxy differently as the reaction model parameter '*m*' is slightly increased emphasizing on the presence of weak interactions between aluminum and epoxy in epoxy/Al composites as been seen in SEM/XRD observations. However, these interactions are almost the same for insulator and conductor composites. A similar fact has been noticed in epoxy/Zn composites that the polymer-metal interactions could be independent of metal concentrations in the polymer [5].

## 5. Conclusion
On the basis of results and discussion, following concluding points are made;

i)   The influence of aluminum on the thermal degradation of epoxy seems complicated in comparison with the influence of zinc on it. This influence is more likely irregular as aluminum may increase the degradation rate of epoxy in the initial stages of reaction; however, at the last stages, its effect is more stabilizing the epoxy. In addition, this effect can be a function of the quantity of aluminum in epoxy. At intermediate stages, the reaction rates might be comparable for pure epoxy and epoxy/Al composites.

ii)  Šestâk Berggren model suggests weak polymer-metal interactions between epoxy and aluminum in epoxy/Al composites.

iii) Complementary analyses (e.g; spectral, structural, etc.) are inevitable with the kinetic study in order to confirm the findings obtained by the kinetic modeling.

**References**

1.  Maaroufi A., Haboubi K., El Amarti A., Carmona F., *J. Mater. Sci.*, 39 (2004) 265.
2.  Bhattacharya S.K., Metal-filled Polymers; Properties and applications, Marcel Dekker, New York, (1986).
3.  Roldughin V.I., Vysotskii V.V., *Prog. Org.Coats,* 39 (2000) 81.
4.  Bruneel E., Ramirez-Cuesta A.J., Driessche I.V., Hoste S., *Phys. Rev.,* 61(B) (2000) 9176.
5.  Arshad M.A., Maaroufi A., Benavente R., Pereña J.M., Pinto G., *Polym. Compos.,* 34(12) (2013) 2049.
6.  Brand J.V..D, Gils S.V., etal., *Prog. Org.Coats,* 51 (2004) 339.
7.  McNamara A.J., Joshi Y., Zhang Z.M., *Int. Jrnl. Therm. Sci.,* 62 (2012) 2.
8.  Guralnick B.W., Seppala J.E., Mackay M.E., *J. Polym. Sci. Pol. Phys.,* 49(11) (2011) 772.
9.  El Homrany M., Maaroufi A., Benavente R., Pereña J.M., Pinto G., *J. Appl. Polym. Sci.,* 118 (2010) 3701.
10. Wan J., Bu Z.-Y., Xu C.-J., Li B.-G., Fan H., *Thermochim. Acta,* 519 (2011) 72.
11. Brown M.E., Gallagher P.K., Handbook of Thermal Analysis and Calorimetry; Recent Advances, Techniques and Applications, Elsevier, B.V. (2008).
12. Flynn J.H., *Thermochim. Acta,* 300 (1997) 83.
13. Friedman H.L., *J. Polym. Sci.,* 6(C) (1964) 183.
14. Vyazovkin S., Burnham A.K., etal., *Thermochim. Acta,* 520 (2011) 1.
15. Flynn J.H., Wall L.A., *J. Res. Nat. Bur. Standards-A Phys. & Chem.,* 70 (1966) 487.
16. Akahira T., Sunose T., *Res. Rep. Chiba. Inst. Technol. (Sci. Technol.),* 16 (1971) 22.
17. Malék J., *Thermochim. Acta,* 200 (1992) 257.
18. Senum G.I., Yang R.T., *J. Therm. Anal. Calorim.,* 11(3) (1977) 445.
19. Lu H., Sun H., Mao A., Yang H., Wang H.,  Hu X., *Mat. Sci. and Eng.; A,* 406(1) (2005) 19.
20. Aufray M., Roche A.A., *Int. J. Adhes. Adhes.,* 27(5) (2007) 387.
21. Denq B.-L., Chiu W.-Y., Lin K.-F., Fu M.-R.S, *J. App. Polym. Sci.,* 81(5) (2001) 1161.
22. Murty M.V.S., Grulke E.A., Bhattachatyya D., *Polym. Degrad. Stab.,* 61 (1998) 421.
23. Zhou W., Yu D., *J. App. Polym. Sci.,* 118(6) (2010) 3156.
24. Arshad M.A., etal., unpublished results.
25. Seo J.G., Youn M.H., Chung J.S., Song I.K., *J. Ind. Eng. Chem.,* 16 (2010) 795.
26. Takahashi Y., Azumi T., Sekine Y., *Thermochim. Acta,* 139 (1989) 133.
27. Tan G., Wang Q., etal.*, J. Phys. Chem.- A*, 115(22) (2011) 5517.
28. Wan J., Li B.-G., Fan H., Bu Z.-Y., Xu C.-J., *Thermochim. Acta,* 511 (2010) 51.
29. Vyazovkin S., Sbirrazzuoli N., *Macromol. Rapid Commun.,* 27(18) (2006) 1515.
30. Chrissafis K., Paraskevopoulos K.M., Bikiaris D., *Thermochim. Acta,* 505 (2010) 59.
31. Montserrat S., Màlek J., Colomer P., *Thermochim. Acta,* 313(1) (1998) 83.
32. Šestak J., Bergren G., *Thermochim. Acta,* 3 (1971) 1.
33. Šimon P., *Thermochim. Acta,* 520 (2011) 156.
34. Brown M.E., *Thermochim. Acta,* 300 (1997) 93.

(2014) ; http://www.jmaterenvironsci.com